

Degradation and Characterization of Antimisting Kerosene

R.J. Mannheimer*

Southwest Research Institute, San Antonio, Texas

The effect of elongational flow on polymer degradation has been studied by forcing antimisting kerosene (AMK) through metal screens and packed tubes at high velocities. At a specific power of 15 kW-s/liter, AMK exhibits filtration and ignition properties similar to Jet A in small-scale tests. A glycol/amine carrier fluid developed to promote rapid dissolution of FM-9 polymer in Jet A has been found to increase antimisting effectiveness, reduce gel formation and filtration resistance, and require less degrader power. Other fuel-soluble hydrogen bonding agents produce similar effects with FM-9 in Jet A. At low Reynolds numbers, the flow of AMK through metal screens and paper filters is characterized by a critical velocity that depends on polymer degradation, filter material, pore size, and the presence of hydrogen bonding agents. Below this critical velocity, the flow resistance of AMK is determined by the low shear viscosity. At a slightly higher velocity, the flow resistance increases dramatically. While this phenomenon is commonly observed with many polymer solutions, in the case of FM-9 it is also associated with gel formation that may result in filter plugging. However, at very high velocities, gel formation and filter plugging are no longer evident with either metal screens or packed tubes.

Nomenclature

A	= area of filter
AMK	= antimisting kerosene
D	= diameter
dp	= bead size
FR	= filtration ratio (filtration velocity of Jet A relative to AMK)
(FR) _i	= initial filtration ratio (undegraded AMK)
k	= permeability
L	= length of tube
Q	= flow rate
Re	= Reynolds number through porous media = Vdp/η
$V = Q/A$	= superficial velocity
VR	= viscosity ratio of AMK relative to Jet A
(VR) _i	= initial viscosity ratio (undegraded AMK)
ΔP	= pressure drop
μ	= shear viscosity
η	= kinematic viscosity

Introduction

ANTIMISTING kerosene (AMK) fuel contains a high molecular weight polymer (FM-9, a proprietary polymer provided by ICI Americas, Inc.) that resists the formation of small droplets and has been shown to improve fire safety in simulated tests of ground crash conditions^{1,2}; however, poor fuel filtration and atomization characteristics preclude its use in aircraft turbine engines and fuel systems until acceptable means of restoring these essential fuel properties can be developed.

While both shear and elongational effects can contribute to polymer degradation, it is expected that elongational flows will be more destructive than shear flows.³ Some insight for this expectation can be provided by considering the differences between these two types of flows (Fig. 1). The familiar shear flow that is commonly produced in a long capillary tube is characterized by a velocity gradient that is normal to the direction flow. As a dilute or semidilute polymer solution flows through the capillary, polymer

molecules tend to be stretched along the principal axis of stress. However, shear flows are rotational; consequently, very little polymer deformation occurs with a low viscosity solvent even at high rates of shear. Elongational flows occur in many practical situations, such as in the entrance region to a capillary tube, in flow through an orifice, and in porous media. In all these examples, the velocity gradient is in the direction of flow. Since this type of flow is irrotational, a polymer molecule would stay oriented in the stress field longer; therefore larger polymer deformations should occur.

Because of the presence of solid boundaries, most flows are a combination of both shear and elongation; however, by an appropriate choice of geometry, one type of flow can be made to dominate. For example, laminar flow in a long capillary tube is primarily a shear flow except for the entrance region. On the other hand, in a very short tube ($L/D < 1$) or for a tube filled with beads, the flow is predominantly elongational.⁴

Since elongational flow is expected to be more effective in producing polymer degradation than shear flow, the primary objective of this work is to determine the effect of the sudden acceleration produced by flow into the pores of metal screens or tubes packed with beads on the mist ignition and filtration properties of AMK. However, relatively few standard tests have been found to be useful in measuring the performance characteristics of AMK; therefore a second but equally important part of this work is the development of test methods that relate to mist flammability and rheological properties of AMK.

Polymer Degradation Experiments

Polymer degradation experiments were conducted by displacing AMK (~6 liters) from a large bore (12.7-cm) hydraulic cylinder (Fig. 2). A high-pressure variable flow pump forced hydraulic fluid into the piston side of the cylinder, forcing the AMK to flow through the metal screens or packed tubes. The volumetric flow rate (Q) was the independent variable and was generally increased from a low value to the highest value (this was limited either by the maximum pressure of 4000 psi or by the maximum flow rate of 5 gal/min) and then back to an intermediate flow rate. This procedure was used to help detect hysteresis effects that might occur owing to filter plugging. The pressure drop (ΔP) was measured with a gage and transducer, with the output of the latter recorded as a function of flow time. Since the pressure drop is a measure of specific degrader power, it has been

Presented as Paper 81-1423 at the AIAA/SAE/ASME 17th Joint Propulsion Conference, Colorado Springs, Colo., July 27-29, 1981; submitted Aug. 6, 1981; revision received June 14, 1982. Copyright © American Institute of Aeronautics and Astronautics, Inc., 1981. All rights reserved.

*Staff Research Scientist, Energy Systems Research Division.

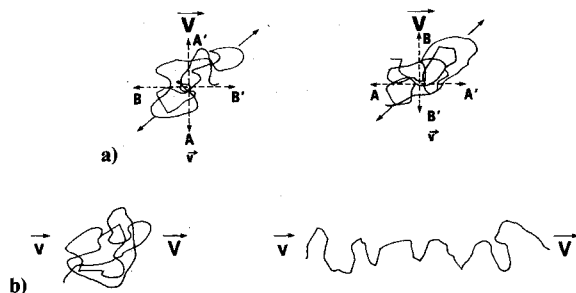


Fig. 1 Illustration of steady shear flow (a) and accelerative (elongational) flow (b).

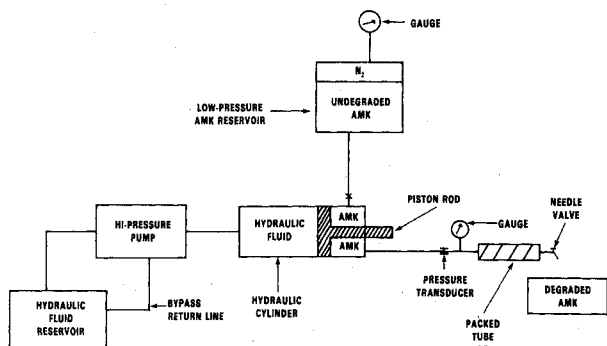


Fig. 2 Sketch of mechanical degrader.

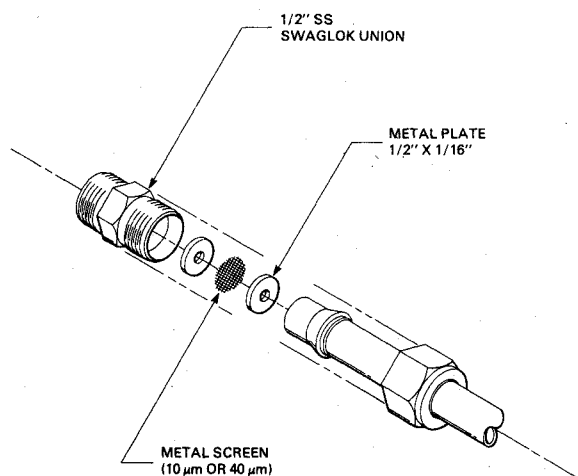


Fig. 3 Metal screen degrader.

expressed in terms of kW-s/liter instead of psi (1.0 psi = 0.0069 kW-s/liter).

Metal screens [(M-8656 (nominal 40 μm) and M-7211 (nominal 10 μm), stainless steel, Dutch weave, Purolator Inc., Newbury Park, California)] (Fig. 3) were held in place by two metal disks (1/2 x 1/16 in.) that fit into a 1/2-in. union. The exposed areas of the screens were determined by the size and number of holes in the disks. Stainless steel tubes (1/4 in.) were packed with uniform glass beads (Fig. 4) (Ferro Microbeads, Jackson, Mississippi). A 1/4-in. union was drilled out to allow it to be fitted with a 1/4-in. tube (0.2-1.9 cm in length). Metal screens (100 mesh) were placed at both ends of the tube to retain the beads, and a backup plate was used to support the screen on the downstream side. Polymer degradation was measured in terms of changes in the viscosity ratio (VR) of AMK relative to Jet A at 40°C, as determined by ASTM D 445. The use of the viscosity ratio as a measure of degradation is based on the relationship between intrinsic viscosity and molecular size or weight.⁵

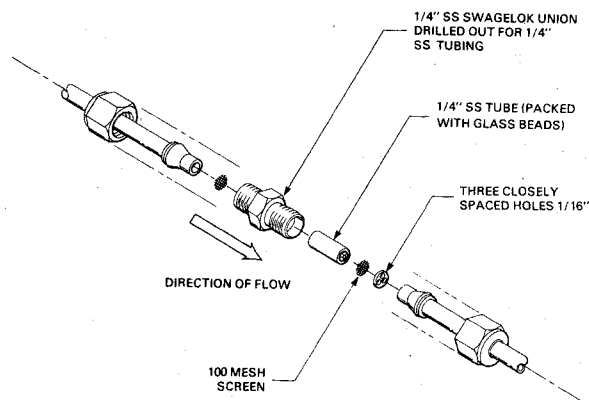


Fig. 4 Packed tube degrader.

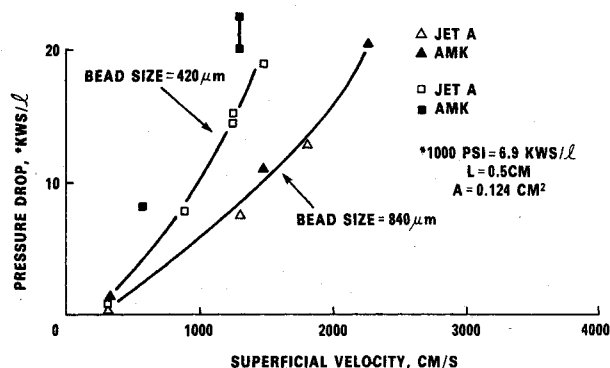


Fig. 5 Flow of AMK and Jet A through packed bed.

The flow of AMK and Jet A through tubes packed with 420- and 840- μm beads at high superficial velocities is shown in Fig. 5. With the larger beads, there was no significant difference in the flow resistance of AMK and Jet A; and with the smaller beads, the flow resistance of AMK was only slightly higher than Jet A. In view of the higher viscosity of AMK [i.e., the viscosity of AMK is approximately 1.7 times that of Jet A at low shear rates ($<2000 \text{ s}^{-1}$) and may be 10 to 12 times that of Jet A at high shear rates], these results may seem unusual. However, the fact that no effect of viscosity was observed in these experiments can be attributed to the high Re flow regime. For example, inertial effects in packed tubes start to become important when $Re > 10$. Since the results in Fig. 5 are representative of $Re > 1000$ (based on the low shear viscosity of AMK), the flow resistance at these conditions would be expected to be due to inertial rather than viscous effects. The absence of gel formation and filter plugging that is characteristic of AMK at low velocities (see Fig. 20) is more difficult to explain; however, it is expected that the average residence time in the packed tube of approximately 0.5 ms [i.e., $t \sim (0.5 \text{ cm}) / (1000 \text{ cm/s})$] or less could be too brief for gel formation to occur. The effects of increasing the tube length for a fixed bead size (840 μm) are summarized in Figs. 6-8. At a given velocity (Fig. 7), a higher degree of degradation (lower viscosity ratio) can be produced by increasing the tube length. On the other hand, the increased degradation in the longer tubes is counterbalanced by the requirement of a higher specific degrader power (Fig. 8).

The relative effectiveness of packed tubes and screens are compared in Fig. 9. The results in Fig. 9 show the level of degradation (characterized by the viscosity ratio), is primarily a function of the specific degrader power (ΔP), and is independent of the bead size or screen size. It will be shown that this result is in good agreement with mist flammability experiments but not with filtration experiments. It is also important to point out that the data in Fig. 9 are representative

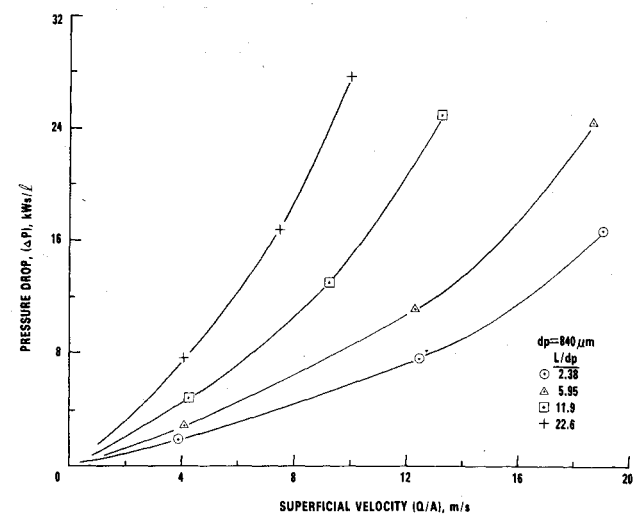


Fig. 6 Flow of AMK through different length packed tubes.

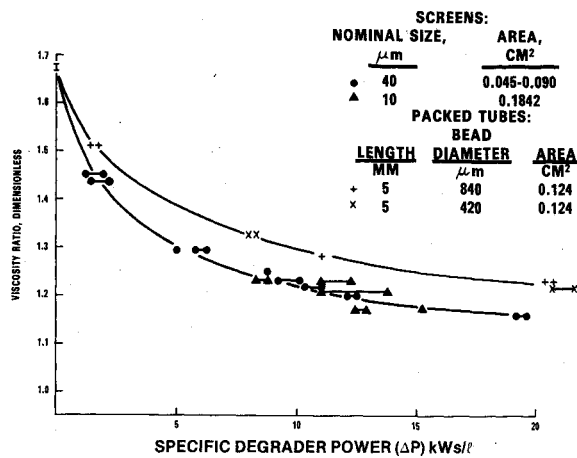


Fig. 9 Power requirement for flow degradation of AMK.

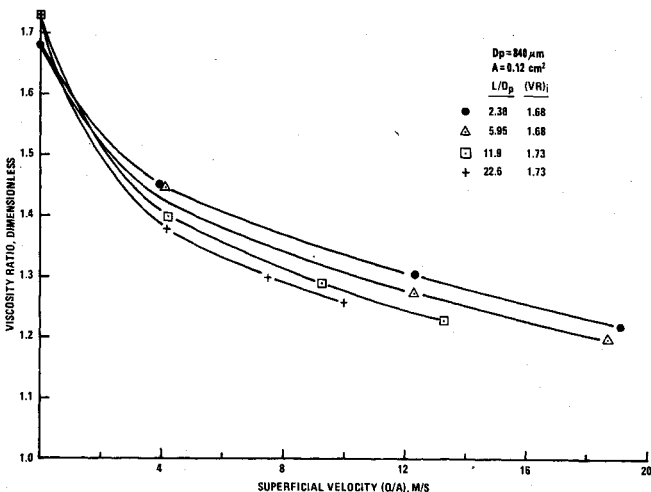


Fig. 7 Effect of tube length and superficial velocity on the viscosity ratio.

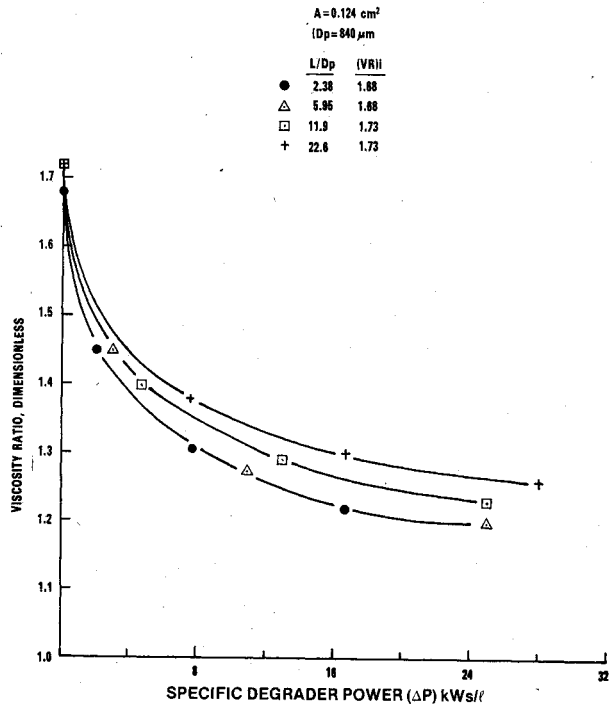
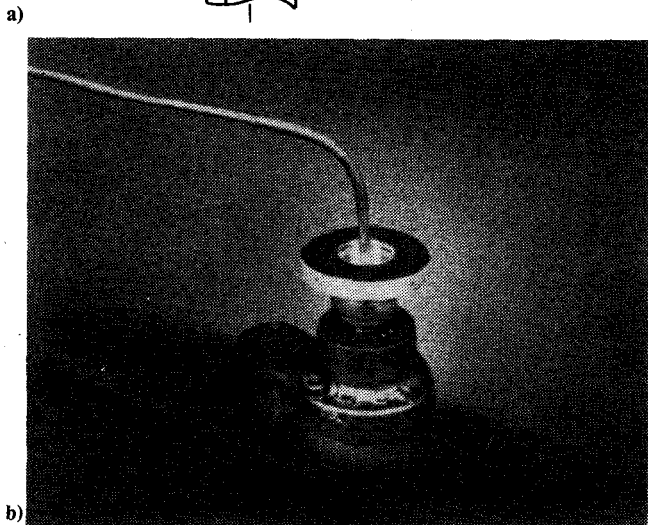
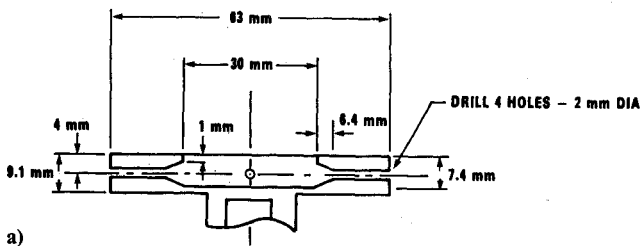


Fig. 8 Effect of tube length (L/d_p) and specific power (ΔP) on viscosity ratio (VR).

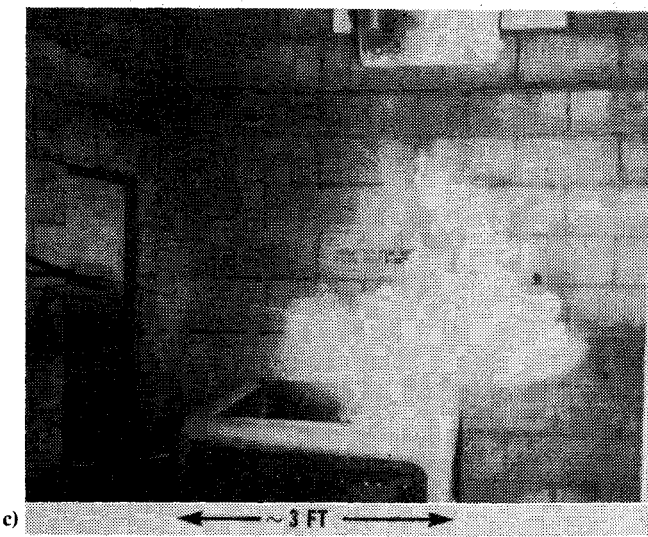


Fig. 10 Mist ignition (spinning disk) apparatus: a) cross-section of disk; b) fuel flows into cavity; c) velocity of disk produces ignitable fuel mist.

of a wide range of flow rates; consequently, these results indicate that the same level of degradation can be achieved at both low and high flow rates by maintaining the same pressure drop or specific power. This result is of particular importance in that a practical degrader must be able to handle fuel flow rates corresponding to both extremes of idle and takeoff fuel flow rates.

In addition to these important findings, the slightly higher efficiency (i.e., lower specific power) of the screens suggested that a simple orifice such as a partially opened needle valve could degrade AMK. Recent experiments have substantiated that a needle valve is a very effective means of producing polymer degradation. In addition, the needle valve has two advantages over the use of screens or packed tubes, i.e., the ability to accommodate different flow rates at constant specific power and less likelihood of plugging due to dirt or other fuel contaminants.

Mist Ignition Experiments

A spinning disk atomizer has been used to measure the resistance of AMK to form an ignitable fuel mist (Fig. 10). Four radially spaced 2-mm-i.d. holes are provided as fuel passageways (Fig. 10a). Fuel flows into the central cavity in the disk head, and a oxyacetylene ignition source is approximately 10 cm from the edge of the disk (Fig. 10b). As the rotational speed of the disk is increased, the fuel contacts the air at a higher relative velocity. Eventually, a velocity is reached at which ignition and flame propagation begins to occur (Fig. 10c). A broad spectrum radiometer is used to measure the effect of disk speed on flame propagation in the fuel mist. It is important to keep in mind that, with the spinning disk atomizer, the tangential component of velocity of the fuel is much higher than the radial component of velocity. Thus the velocity of the fuel relative to the surface of the fuel passage is low, and this should minimize any mechanical degradation from occurring before the AMK contacts the air.

In order to rapidly dissolve the FM-9 polymer in Jet A, a carrier fluid consisting of a fuel-soluble glycol and amine was developed by ICI Americas, Inc. Mist flammability data for standard AMK (0.3% FM-9 + carrier fluid in Jet A) degraded at different power levels and with different sized beads are presented in Fig. 11. Below a velocity of 72 m/s, flame propagation of undegraded AMK is negligible compared to Jet A. However, at higher velocities, flame propagation increases with disk velocity. It is important to note that the critical disk velocity is close to the pass/marginal air velocity for AMK in fuel spillage tests conducted at the FAA Technical Center. At low degrader power (from 3 to 4 kW-s/liter), the critical disk velocity is only slightly lower than undegraded AMK; however, at 15 kW-s/liter and higher, the mist flammability of AMK is indistinguishable from Jet A.

Experiments were also conducted to determine the effect of the carrier fluid on mist ignition resistance and specific degrader power required to eliminate mist ignition resistance (Fig. 12). The critical velocity of undegraded AMK without carrier fluid is from 15 to 20 m/s lower than standard AMK. This finding appears to be substantiated by large-scale flammability tests.^{1,2} Furthermore, AMK without carrier fluid is more resistant to mechanical degradation. For example, at a power level of from 3 to 4 kW-s/liter, the critical velocity of AMK with carrier fluid was reduced from 73 to between 48 to 52 m/s. In contrast, at power levels up to 8 kW-s/liter, the critical velocity of AMK without carrier fluid remained essentially unchanged. Furthermore, at a power level of 15 kW-s/liter or greater, the mist flammability of AMK without carrier fluid required 24 kW-s/liter to achieve this condition. The increased resistance to mechanical degradation of AMK made without carrier fluid can be attributed to the fact that the FM-9 polymer is in a much tighter coil without the solubilizing effect of the carrier fluid and is therefore more difficult to degrade.

Filtration Experiments

A standardized filtration test developed by the Royal Aircraft Establishment (RAE) was used to measure intentional degradation. Basically, this test measures the time for a specific volume (96 ml) of fuel to flow between two timing marks on a vertically mounted glass tube (2.5 cm i.d.). A 16-18- μ m Dutch weave screen is attached to the bottom of the tube, and the flow time for AMK relative to Jet A is reported as the filtration ratio (FR). For undegraded AMK at 25°C, this ratio is generally between 40 and 50; however, degradation can reduce this ratio to close to 1.0.

The effect of bead size on polymer degradation as measured by the filtration ratio is shown in Fig. 13. The lowest filtration ratio for fuel degraded with the 840- μ m beads was 2.0. Increasing tube length generally lowers the superficial velocity required to produce the same filtration ratio; however, as with the viscosity ratio, a longer tube requires a higher specific degrader power.

Similar experiments were conducted with smaller glass beads (420 μ m) and two different length tubes. Except for one important difference, the results of these experiments are in good agreement with those obtained with the larger beads (840 μ m). This difference suggests that degradation is more efficient with smaller beads. For example, the results of tube length on the specific degrader power required to reduce the viscosity ratio to a particular value was almost identical for both sized beads. However, the effect of bead size on filtration ratio was significant. In particular, the specific degrader power required to produce a filtration ratio of 2.0 was approximately twice as high for the larger beads (24 kW-s/liter compared to 12.5 kW-s/liter). As was seen earlier, there was no significant effect of bead size on the viscosity ratio or the critical ignition velocity (Figs. 9, 11, and 12). In an attempt to understand the reasons for these differences, experiments were undertaken to determine the physical significance of the filtration ratio test.

The laminar flow of dilute polymer solutions through porous media is often characterized by two distinctly different flow regimes.^{4,6} Below a critical strain rate, the flow resistance is determined by the shear viscosity; however, at higher rates of strain the flow resistance increases dramatically and can become orders of magnitude higher than the shear viscosity. This high-resistance flow regime is a viscoelastic phenomenon associated with the elongational flowfield that is characteristic of porous media. Because of the gel-forming tendency of the FM-9 polymer, it is difficult to differentiate between this inherent viscoelastic phenomenon and filter plugging with the standard filtration test. Consequently, more detailed experiments were conducted by maintaining a fixed gas pressure over a fluid reservoir and collecting a quantity of filtrate over a timed interval. This procedure is similar to the filtration ratio test, but it has several important advantages. For example, by measuring the flow rate or velocity at different pressures, more information can be obtained on the rheological behavior of AMK. Also, by making measurements at increasing and decreasing pressures, effects of filter plugging can be easily detected.

The results in Fig. 14 demonstrate the flow characteristics of Newtonian liquids, in this case Jet A and diesel fuel. Measurements were taken at increasing and decreasing pressures to detect filter plugging. It is interesting to note that the superficial velocity for Jet A at a pressure head of 20 cm is approximately 4 cm/s. This is close to the average superficial velocity of 4.4 cm/s for Jet A in the standard filtration test. This illustrates the similarity in flow conditions between the standard filtration test and this experiment. While the average superficial velocity (\bar{V}) is not reported in the standard filtration test, it can be calculated from the fuel volume (96 ml) and screen area (4.5 cm²); i.e., $\bar{V} = 21.3/t$, where t is the flow time in seconds.

The linear flow characteristics shown in Fig. 14 are

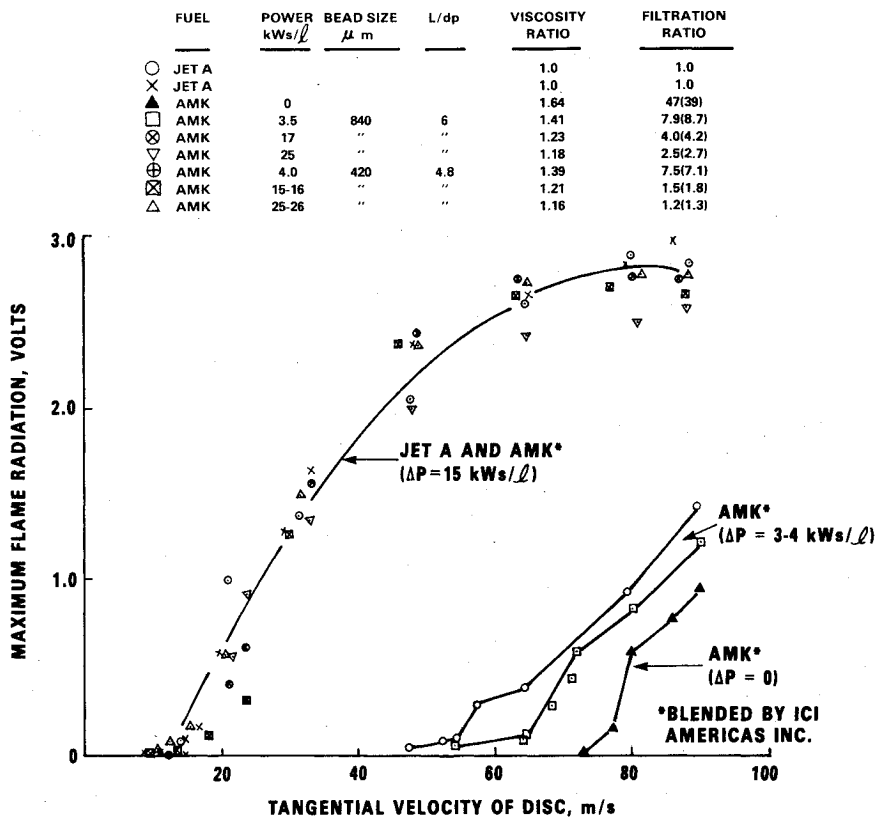


Fig. 11 Effect of degradation on mist flammability of AMK.

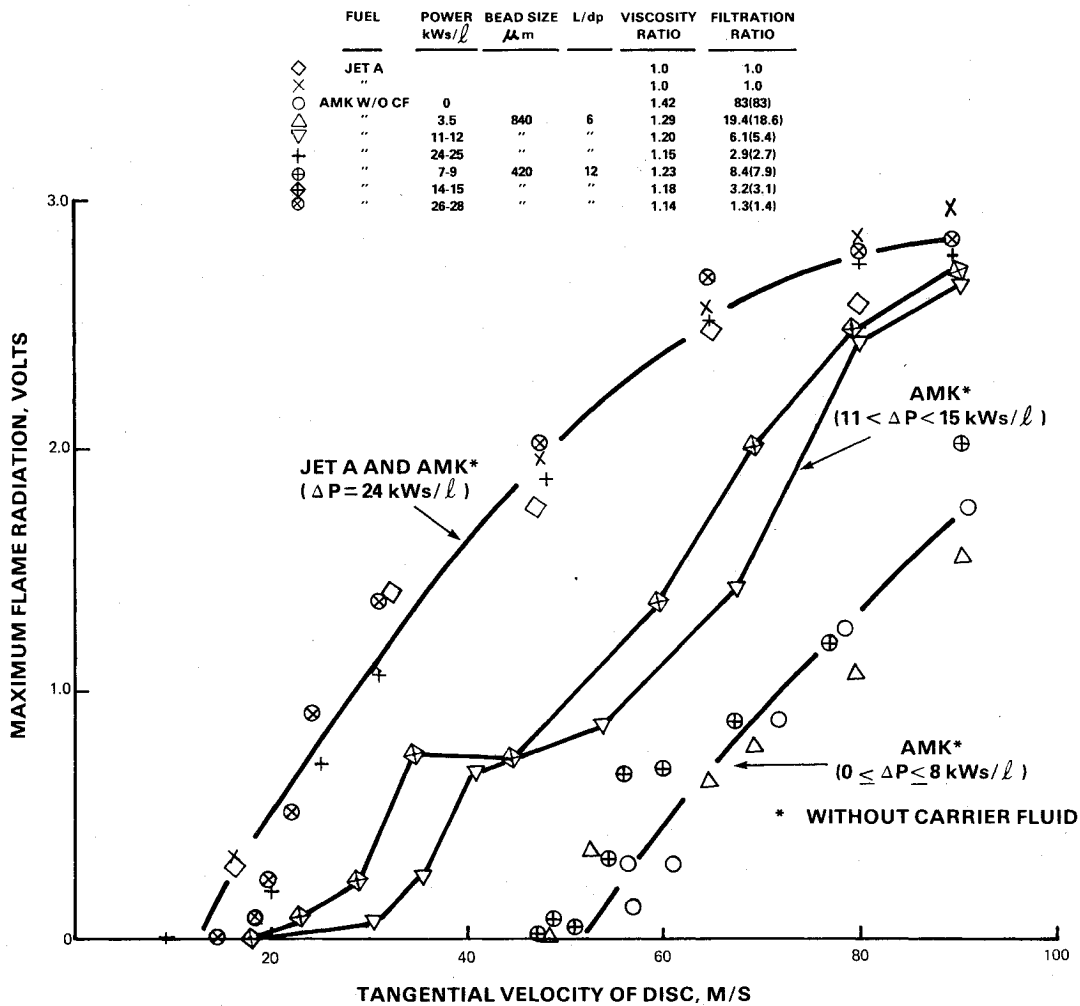


Fig. 12 Effect of degradation on mist flammability of AMK without carrier fluid.

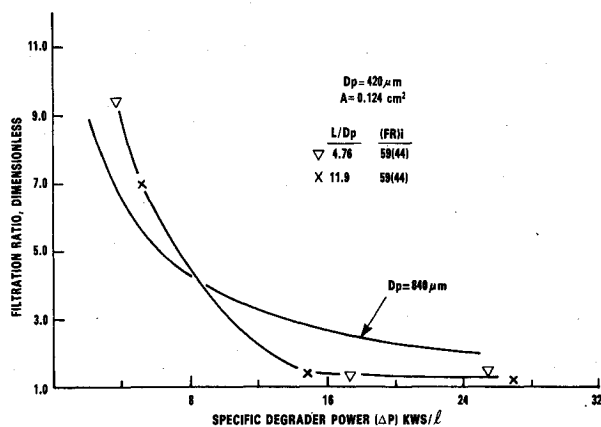


Fig. 13 Effect of tube length (L/dp) and specific power (ΔP) on filtration ratio (FR).

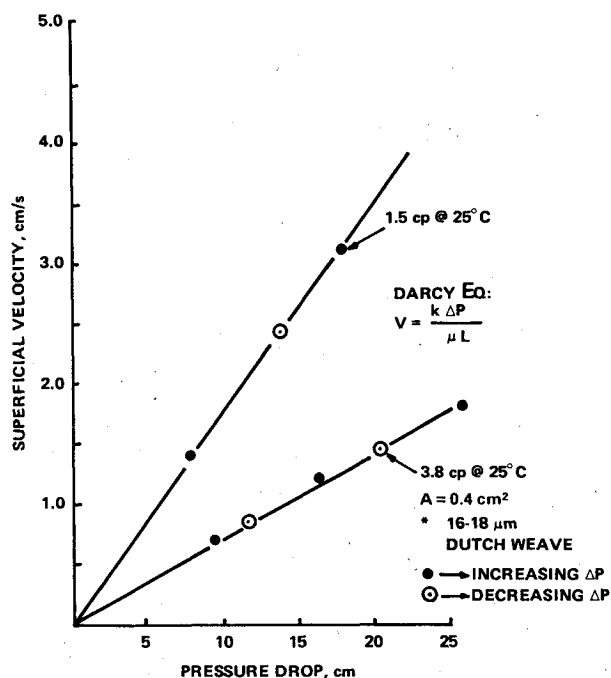


Fig. 14 Effect of pressure drop on superficial velocity of Newtonian liquids through metal filters.

representative of the laminar flow regime in which the Darcy equation appears to be valid:

$$V = k \Delta P / \mu L \quad (1)$$

where $V = Q/A$ is the superficial velocity, ΔP is the pressure drop, L is the filter thickness, μ is the absolute (shear) viscosity, and k is the permeability.

More general relationships for non-Newtonian behavior have been derived,⁷ but for now this simple relation will be used. Since the permeability is a function of several factors such as pore size, pore shape, and porosity or void fraction, the following comments will refer to a specific filter configuration, i.e., 16-18- μ m, stainless steel, Dutch weave. In this case, the Darcy equation predicts that the velocity ratio of Jet A relative to diesel fuel (i.e., the filtration ratio) will be $3.8/1.5 \text{ cP} = 2.53$. This is very close to the measured value shown in Fig. 14. Thus, while there is a large difference between the filtration ratio (40 to 50) and viscosity ratio (1.65 to 1.75) for undegraded AMK, the Darcy equation predicts that these two measurements will have a common asymptote (i.e., $FR \rightarrow VR$) for highly degraded AMK. Furthermore, this result demonstrates that the standard filtration test is basically a viscometer. Filtration measurements for two

Table 1 Filtration measurements for two highly degraded samples of AMK

Viscosity ratio	Filtration ratio		
	16-18- μ m metal	20- μ m paper	10- μ m paper
1.17 ^a	1.1 (1.2)	8.6 (13.6)	27 (32)
1.22 ^b	1.3 (1.2)	3.4 (3.2)	33 (33)

^aFM-9 with carrier fluid in Jet A, 25 kW-s/liter—SwRI degrader. ^bFM-9 with carrier fluid in Jet A-1, 100 kW-s/liter RAE degrader.

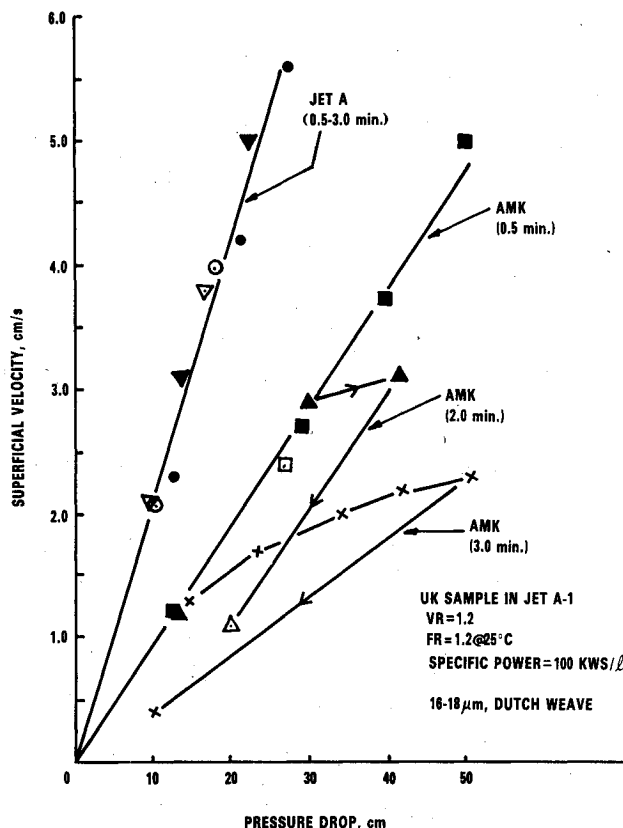


Fig. 15 Effect of pressure drop and flow time on the superficial velocity of highly degraded AMK through metal filters.

highly degraded samples of AMK (see Table 1) substantiate this prediction for a 16-18 μ m screen but not for paper filters.

If these samples were fully degraded, the filtration ratio should be the same value as the viscosity ratio regardless of the filter material. Consequently, the increasing filter ratio with decreasing filter size indicates that the standard filtration test, which specifies a 16-18- μ m metal screen, overestimates the level of polymer degradation. This sensitivity of paper filters to plugging by partially degraded AMK is probably due to at least three factors: 1) the pore size and shape distribution of a paper filter is broader than a metal screen; 2) the effective open area of a paper filter is less than a metal screen (this results in higher local velocities); and 3) a metal screen is only one pore deep, while a paper filter has an effective depth of several pores. This last factor is particularly important in that gel formation occurs after AMK flows through the first pore. This results in the gel forming on the downstream side of a metal screen; however, gel forms inside a paper filter and this results in rapid plugging.

It was suspected that part of the problem with the standard filtration ratio test was the very short flow time (approximately 4 to 5 s) available for gel formation. In order to test this hypothesis, filtration experiments were conducted with Jet A and a highly degraded AMK sample ($VR=1.2$, $FR=1.2$) at different pressure gradients and for different flow times. This particular AMK sample was degraded by the

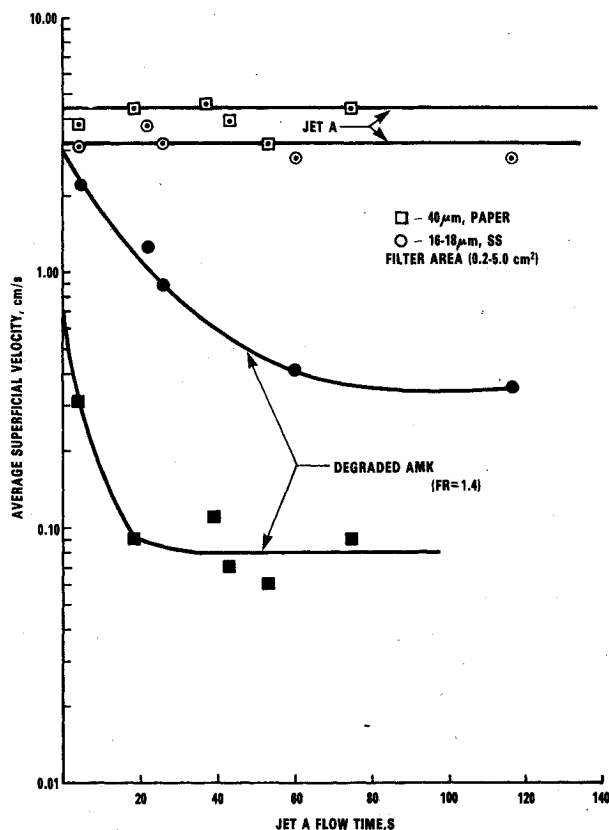


Fig. 16 Effect of flow time (area) on filtration velocity of degraded AMK in two different filters.

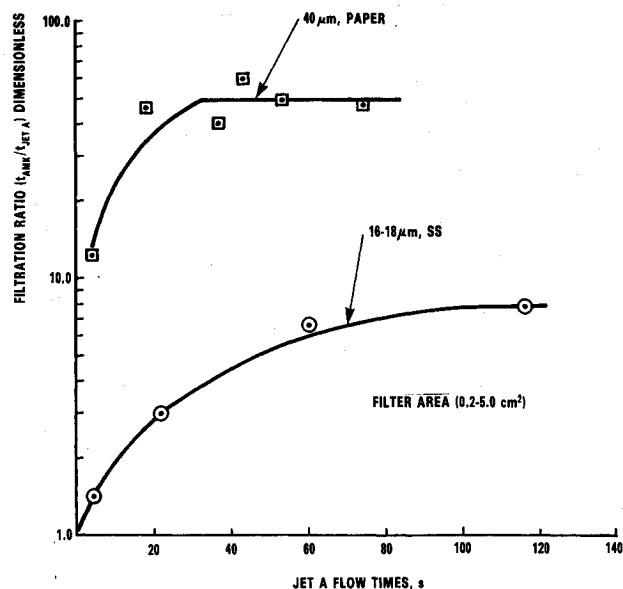


Fig. 17 Effect of flow time (area) on filtration ratio of degraded AMK in two different filters.

RAE. The results of these experiments (Fig. 15) show no effect of flow time on the velocity of Jet A over the range of from 0.5 to 3.0 min. However, different results were observed for the degraded AMK depending on the flow time. For relatively short times of 30 s or less, the superficial velocity of the degraded AMK increased linearly with increasing pressure. For a flow time of 2 min, a critical velocity is evident at 3 cm/s, and at a flow time of 3 min, the critical velocity was close to 1 cm/s. The hysteresis loops for flow times above 2 min clearly indicate that the critical velocity is associated with gel formation and filter plugging.

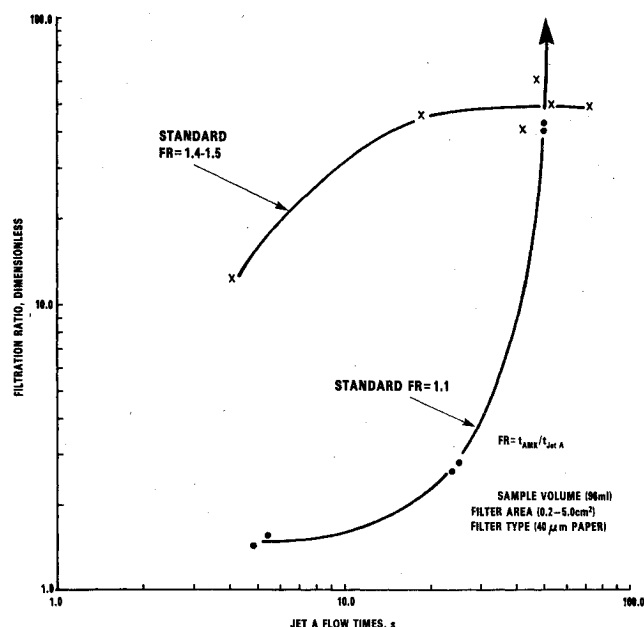


Fig. 18 Effect of Jet A flow time on filtration ratios of degraded AMK.

These results confirmed that the filtration ratios in the standard test were low owing to the relatively short flow time (4 to 5 s) for this test. Consequently, experiments were conducted in which the flow time in the filtration ratio test was increased by decreasing the cross-sectional area of the filter. This was achieved by placing the filter paper or screen between two disks that had a hole of the desired size in the center. Data were obtained for areas from 5.0 cm² (standard filtration ratio test) down to 0.2 cm². The flow time was first measured for Jet A and then AMK, and each filtration ratio was obtained with a fresh filter paper. Since the time for the flow of 96 ml of Jet A increased inversely with the filter area, the average velocity ($V = Q/A$) remained essentially constant at 4.5 cm/s. On the other hand, the velocity of degraded AMK samples generally decreased with increasing flow time or decreasing area.

The results in Fig. 16 were obtained with a degraded sample of AMK ($FR = 1.4$) and two different types of filter material (i.e., the standard 16-18- μ m screen and 40- μ m paper used in the JT8D main fuel filter). These results show that while the velocity of Jet A is independent of the flow time or area, the velocity of degraded AMK decreases with increasing Jet A flow time (i.e., decreasing area). While this phenomenon occurs with both metal screens and paper filters, it is evident that the limiting filtration velocity is reached sooner with the paper filter. These same results are presented in Fig. 17 in terms of filtration ratios instead of filtration velocities. Since paper filters are more sensitive to plugging, one might conclude that the filtration ratio test could be improved by the use of paper filters instead of metal screens. However, data for two different samples of degraded AMK show that results can depend on the filter area of flow time even with paper filters (Fig. 18). One sample is characterized by a room temperature filtration ratio of 1.4 to 1.5 with a 16-18- μ m screen. Since the filtration ratio of this sample with the 40- μ m paper filter is almost an order of magnitude higher, it is evident that this sample is not highly degraded. As the filter area is reduced, the filtration ratio at first increases and then approaches a limiting value (~ 47).

The second sample is characterized by a filtration ratio of 1.1 with the standard 16-18- μ m screen and by a filtration ratio of 1.5 for a 40- μ m paper filter. This is almost an order of magnitude lower than the previous sample. This low filtration ratio would suggest a very high degree of degradation. Unfortunately, when measurements were made with different

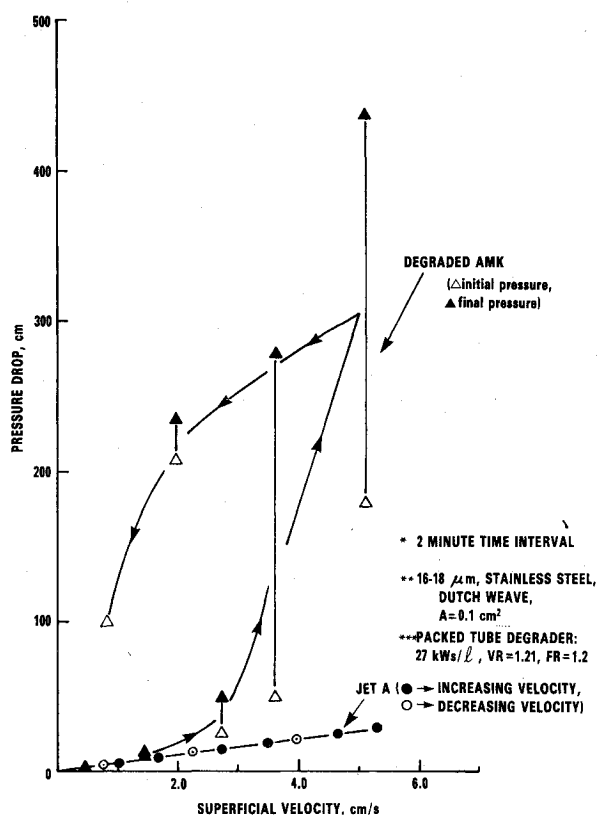


Fig. 19 Effect of superficial velocity on pressure drop (2-min time interval) across a 16-18- μ m, stainless steel, Dutch weave filter ($A = 0.1 \text{ cm}^2$) with Jet A and degraded AMK (packed tube degrader: 27 kWt/l, $VR = 1.21$, $FR = 1.2$).

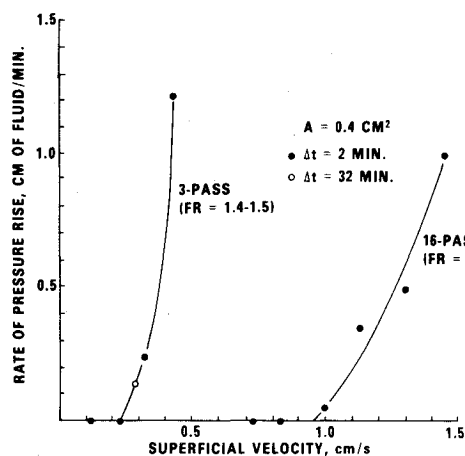


Fig. 20 Filter plugging characteristics of degraded AMK (JT8D fuel pump) with 40- μ m (Pratt & Whitney) paper filters.

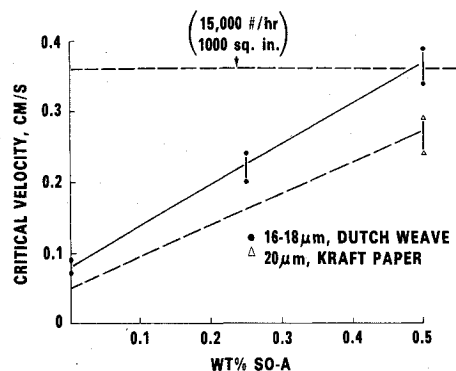


Fig. 21 Effect of surfactant on the critical filtration velocity of undegraded AMK.

filter areas, the filtration ratio increased, and eventually surpassed that of the first sample. These results demonstrate that filtration ratios, as measured by the filtration apparatus that is currently in general use, can result in serious errors regarding degradation, even if the metal screens are replaced by paper filters. While it is possible to obtain a better estimate of the filtration ratio by decreasing the area, this approach is very tedious.

The results of these experiments confirm that the flow time (4 to 5 s) in the standard filtration test is too short to detect gel formation with highly degraded AMK. Although the previously described experiment is capable of detecting these effects, the time-dependent nature of this phenomenon suggested the need for a filtration test that more closely simulated flow conditions in an aircraft fuel delivery system, and in particular, one that is able to measure flow resistance as a function of time.

In the pump filtration test, a gear pump (0-100 rpm) and drive transmission are used to force fuel through a filter at different flow rates. The pressure drop across the filter is measured as a function of time by a transducer and strip chart recorder. For the following experiments, the flow time was held constant at 2 min. Experiments conducted with Jet A (Fig. 19) showed no measurable increase in pressure over the 2-min interval. Furthermore, the pressure drop increased linearly with increasing superficial velocity (which is characteristic of laminar flow of a Newtonian liquid), and there was no evidence of hysteresis when the velocity was decreased. It is also important to note that at a velocity of 4 cm/s, the measured pressure drop was 20 cm; and that this is close to the average pressure drop that results in a velocity of from 4 to 5 cm/s for Jet A in the standard filtration test.

Significantly different experimental results (Fig. 19) were obtained with what should have been highly degraded AMK, as evidenced by the filtration ratio of 1.2 at 25°C. In this case, the pressure drop remained independent of time as long as the velocity was below 1 cm/s. It is important to note that the value of the filtration ratio is equivalent to an average velocity in the standard filtration test of close to 4 cm/s. At higher velocities, the pressure drop increased linearly with time after a short induction time. This effect of increasing pressure with time is illustrated by the separation of the open and closed data points at a fixed velocity. The rate of pressure rise with time was significantly higher as the superficial velocity increased above 1 cm/s. While this effect appeared to be reversible in that the pressure drop was independent of time when the velocity was reduced below 1 cm/s, the hysteresis loop is definite evidence of filter plugging (i.e., $\Delta P = 5 \text{ cm}$ at $V = 0.9 \text{ cm/s}$ for V increasing and $\Delta P = 100$ at $V = 0.9 \text{ cm/s}$ for V decreasing).

The pump filtration test is currently being used to estimate the conditions for which AMK will flow through a filter without plugging. The critical velocity is determined by the highest velocity at which the pressure drop across the filter remains constant for 2 min. The results in Fig. 20 show that two samples of degraded AMK that have close to the same filtration ratio have critical filtration velocities that are significantly different. These samples were degraded by Pratt & Whitney Aircraft by recirculating the AMK through a JT8D engine fuel pump.⁸

Pump filtration experiments were also conducted to determine the effect of a surfactant (SO-A, Scher Chemicals, Inc.) on the critical filtration velocity of undegraded AMK. The results in Fig. 21 show that the critical filtration velocity increases in direct proportion to the amount of surfactant added over the range of from 0 to 0.5 wt.%. At a concentration of 0.5% surfactant, undegraded AMK is able to flow through a 16-18- μ m Dutch weave screen at velocities equivalent to takeoff conditions (Fig. 21). It is important to mention that while the surfactant obviously reduces gel formation and improves the filterability of AMK, it does not appear to adversely affect fire safety. This result makes it

difficult to attribute the mist fire resistance of FM-9 to its gel-forming characteristics.

Conclusions

1) AMK can be degraded by high velocity flow through metal screens or packed tubes without significant plugging due to gel formation. At a specific power of 15 kW-s/liter (30 h.p. at 10,000 lb/h), AMK exhibits filtration and ignition properties similar to Jet A in small-scale tests.

2) The level of degradation (characterized by the viscosity ratio or the critical ignition velocity) appears to be independent of bead size or screen size and to be a unique function of specific degrader power (ΔP).

3) The spinning disk test characterizes the mist flammability of AMK in terms of a critical velocity below which flame radiation is negligible compared to Jet A. This critical velocity appears to correspond to the pass/marginal air velocity in large-scale fuel spillage tests. Using the critical disk velocity as the primary criterion of fire protection, it appears that i) the glycol/amine carrier fluid increases the effectiveness of FM-9 in Jet A; ii) the addition of hydrogen bonding agents that eliminate the gel-forming tendency of AMK does not adversely affect mist flammability; iii) at a specific degrader power of 15 kW-s/liter and higher, standard AMK has mist flammability characteristics similar to jet A; and iv) AMK without carrier fluid requires more power to degrade than standard AMK.

4) The laminar flow of AMK through filter media is characterized by a critical velocity below which flow resistance is determined by the low shear viscosity. At a slightly higher velocity, gel formation results in filter plugging

in which the pressure drop across the filter increases with time. This critical filtration velocity is a function of the degree of polymer degradation and filter properties, such as pore size and pore geometry.

Acknowledgments

This program was funded by the Department of Transportation under DOT-FA79WA-4310. The work was performed for the Federal Aviation Administration (FAA) under the management of A. Ferrara, Federal Aviation Administration (FAA) under the management of A. Ferrara, Federal Aviation Administration Technical Center. J.L. Jungman and P.J. Gutierrez of Southwest Research Institute performed the experimental measurements and assisted in the data reduction.

References

- ¹San Miguel, A. and Williams, M.D., Report FAA-RD-78-50, 1978.
- ²Klueg, E., 6th U.S./U.K. Technical Committee Meeting on Antimisting Fuel, March 1980.
- ³Bueche, F.J., *Applied Polymer Science*, Vol. 4, 1960, pp. 101-106.
- ⁴Marshall, R.J. and Metzner, A.B., *Industrial and Engineering Chemistry Fundamentals*, Vol. 6, 1967, p. 393.
- ⁵Billmeyer, F.W., *Textbook of Polymer Science*, 2nd ed., Wiley Interscience, New York, 1971, pp. 84-90.
- ⁶Mannheimer, R.J., Report FAA-RD-77-10, 1977.
- ⁷Christopher, R.J. and Middleman, S., *Industrial and Engineering Chemistry, Fundamentals*, Vol. 4, 1965, p. 422.
- ⁸Fiorentino, A., De Saro, R., and Franz, T., Report NASA-CR-16528, 1980.

AIAA Meetings of Interest to Journal Readers *

Date	Meeting (Issue of <i>AIAA Bulletin</i> in which program will appear)	Location	Call for Papers†
1983			
April 11-13	AIAA 8th Aeroacoustics Conference (Feb.)	Terrace Garden Inn Atlanta, Ga.	July/ Aug. 82
May 2-4	24th AIAA/ASME/ASCE/AHS Structures, Structural Dynamics, and Materials Conference (March)	Sahara Hotel Lake Tahoe, Nev.	June 82
May 10-12	AIAA Annual Meeting and Technical Display	Long Beach Convention Center, Long Beach, Calif.	
June 1-3	AIAA/ASCE/TRB/ATRIF/CASI International Air Transportation Conference (April)	The Queen Elizabeth Hotel Montreal, Quebec, Canada	Oct. 82
June 6-11‡	6th International Symposium on Air Breathing Engines	Paris, France	April 82
June 13-15	AIAA Flight Simulation Technologies Conference (April)	Niagara Hilton Niagara Falls, N.Y.	Sept. 82
June 27-29	AIAA/SAE/ASME 19th Joint Propulsion Conference and Technical Display (April)	Westin Hotel Seattle, Wash.	Sept. 82

For a complete listing of AIAA meetings, see the current issue of the *AIAA Bulletin*.

†Issue of *AIAA Bulletin* in which Call for Papers appeared.

‡Meetings cosponsored by AIAA.